

Influence of $\text{Al}_2\text{O}_3 \cdot \text{XH}_2\text{O}$ Crystallinities on the Morphology of AlOOH Whiskers

Meijuan Chen, Lan Xiang*

Department of Chemical Engineering, Tsinghua University, Beijing 100084, China

*Corresponding authors. Email: xianglan@mail.tsinghua.edu.cn

Abstract

γ - AlOOH whisker is one of the most popular precursors for the formation of Al_2O_3 whisker. In this paper, a facile hydrothermal method was developed to prepare γ - AlOOH whiskers, using hydrated alumina with different crystallinity as the hydrothermal precursors. Amorphous hydrated alumina precursors were prepared by mixing HCl and NaAlO_2 at room temperature, while crystalline hydrated alumina precursors were produced by precipitation of NaAlO_2 solution. γ - AlOOH whiskers with a length of 800-1500 nm and a diameter of 20-40 nm were formed by hydrothermal treatment (220 °C, 8.0 h) of the mixing of two kinds of precursors. The experimental results indicated that the different dissolving rates of hydrated alumina precursors were one of the main reasons for the formation of γ - AlOOH whiskers with high aspect ratio.

Keywords: γ - AlOOH whiskers; Crystallinity of precursors; Hydrothermal technology

Citation: M. Chen et al. Influence of $\text{Al}_2\text{O}_3 \cdot \text{XH}_2\text{O}$ Crystallinities on the Morphology of AlOOH Whiskers. *Nano Biomed Eng.* 2010, 2(2), 121-125. DOI: 10.5101/nbe.v2i2.p121-125.

1. Introduction

As one of the most important oxides, Al_2O_3 fibers have been attracted much attention because of their potential applications in catalysts, adsorption, composites and ceramics. The use of Al_2O_3 fibers as strengtheners in ceramics or aluminum matrix composites was of great interest owing to their high melting point, high elastic modulus and stable chemical properties, etc [1-3]. These features make Al_2O_3 fibers advantageous over non-oxide fibers, which lose these properties through oxidation at high temperatures. γ - AlOOH fibers were one of the most widely used alumina precursors in the preparation of Al_2O_3 fibers, and the hydrothermal route was usually used for the controllable formation of AlOOH since AlOOH can be produced in a wide range of synthesis conditions. Many researchers have studied the hydrothermal formation of γ - AlOOH fibers, and found several main factors affected the morphology of γ - AlOOH such as the hydrothermal precursor, hydrothermal pH, template or inducer and so

on. Kaya et al reported the morphological changes of γ - AlOOH at different pH and synthesized the fibrous γ - AlOOH at acidic conditions (pH=2-5), whereas plate-like crystals were synthesized in basic media (pH=10) [4]. The surfactants as the templates or inducers were used to promote the hydrothermal growth of γ - AlOOH whisker. Zhu et al synthesized the porous nanofibers and plate-like AlOOH particles under hydrothermal condition at $\text{PEO}/\text{Al} > 0.47$ and $\text{PEO}/\text{Al} < 0.47$, respectively, via the hydrogen-bond interaction of PEO with the surface hydroxyl groups of the AlOOH nanoparticles [5]. γ - AlOOH fibers with the length of 1-2 μm were obtained by mixing AlCl_3 solution and NaOH solution under NaPa existed ($\text{NaPa}/\text{Al}=0.57$). The problems were that the surfactants were usually harmful to environment and expensive. The length of γ - AlOOH partly depended on the kinds of hydrothermal precursors [6]. He produced the fiber-like cluster AlOOH with a length of 1 μm by treating the obtained

aluminium acetate at pH 2.0, while the fiber-like cluster AlOOH with a length of 200nm obtained by mixing $\text{Al}(\text{NO}_3)_3$ solution with quadrol [7-8]. He et al reported the hydrothermal formation of AlOOH fibers with the length of 1 μm at 240 °C for 16 h under sulphate existed. The hydrothermal precursor was amorphous hydrate alumina prepared by mixing HNO_3 solution and NaAlO_2 solution [9-10].

In this paper, a method by changing the crystallization of hydrothermal precursor to promote the growth of AlOOH fibers was introduced. Amorphous hydrated alumina and crystalline hydrated alumina were prepared from NaAlO_2 solution by different methods. The properties of the two were investigated. The influence of the solution composition on the hydrothermal formation of $\gamma\text{-AlOOH}$ whiskers was also studied. The results revealed that when amorphous hydrated alumina and crystalline hydrated alumina were mixed with different mass ratio, the length of $\gamma\text{-AlOOH}$ was discrepant. The explanation was the two had different solubility in hydrothermal solution. Amorphous hydrated alumina dissolved quicker than crystalline one. Stable solution supersaturation was the impetus of AlOOH according to one dimensional growth.

2. Experimental

2.1 Experimental Procedures

3.0 mol·L⁻¹ NaAlO_2 solution was prepared by dissolving particulate $\text{Al}(\text{OH})_3$ in 10 mol·L⁻¹ NaOH , keeping the molar ratio of Na_2O to Al_2O_3 as 1.25 : 1.0. 3.0 mol·L⁻¹ NaAlO_2 was then added dropwise to 5.0 mol·L⁻¹ HCl at room temperature to obtain amorphous hydrated aluminum. The slurry was then washed by the distilled water to get rid of Cl^- . 3.0 mol·L⁻¹ NaAlO_2 was stirred at 20 °C for 24 h and crystalline hydrated alumina was obtained. Then it was activated by acid treatment with 2 h. Amorphous precursor and crystalline precursor with different mass percentage were mixed and the slurry pH was adjusted to 4.5. Then the mixture was put into a Teflon-lined stainless steel autoclave, heated (4 °C·min⁻¹) to 220 °C and kept in isothermal conditions for 8.0 h. After hydrothermal treatment, the autoclave was cooled down to room temperature naturally and the suspension was filtered, washed with distilled water and dried at 105 °C for 24 h.

2.2 Characterization

The thermal decomposition behaviors and the structures of the samples were investigated by the thermal gravimetric analyzer (STA-409C, Netzsch, Germany) and the powder X-ray diffractometer (D8advance, Bruker, German), respectively. The morphologies of the samples were examined by the field emission scanning electron microscope (JSM 7401F, JEOL, Japan) and the high-resolution transmission electron microscopy (JEM-2010, JEOL, Japan).

3. Results and discussion

3.1 Morphology and Composition of the Hydrothermal Precursors

Fig. 1a shows the XRD pattern and TG curve of the precursor prepared by the reaction of NaAlO_2 and HCl solution. Weak diffraction peaks indicated that it was amorphous. The weight losses of the precursor within 105-1000 °C were 49.6 % which were much higher than the theoretical weight loss (34.6 %) for the conversion of $\text{Al}(\text{OH})_3$ to Al_2O_3 . The precursor was expressed as $\text{Al}_2\text{O}_3 \cdot 5.6\text{H}_2\text{O}$. Amorphous $\text{Al}_2\text{O}_3 \cdot 5.6\text{H}_2\text{O}$ had uneven particle sizes between 200nm and 1500nm (Fig. 2a). Concern was they had porous structures and the porous structures promoted amorphous precursor to dissolve during hydrothermal process. The holes contained adsorbed water which was difficult to remove although in high temperature. The lost of absorbed water and structure water were overlapping, leading to difficult to distinguish.

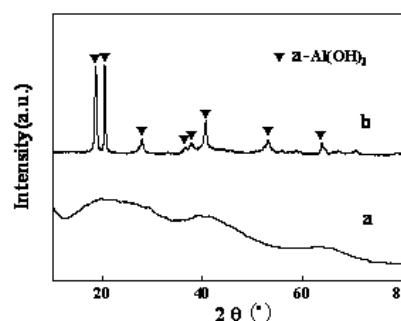


Figure 1. XRD patterns of hydrothermal precursors: (a) amorphous $\text{Al}_2\text{O}_3 \cdot 5.6\text{H}_2\text{O}$; (b) crystalline $\text{Al}_2\text{O}_3 \cdot 3.0\text{H}_2\text{O}$

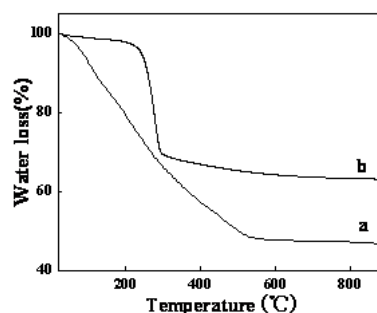


Figure 2. TG curves of hydrothermal precursors: (a) amorphous $\text{Al}_2\text{O}_3 \cdot 5.6\text{H}_2\text{O}$; (b) crystalline $\text{Al}_2\text{O}_3 \cdot 3.0\text{H}_2\text{O}$

Fig. 1 and Fig. 2 shows XRD patterns and TG curves of the precursor prepared by the reaction of HCl and NaAlO_2 and precipitation of NaAlO_2 , respectively. The peak positions indicated that the precursor prepared by precipitation of NaAlO_2 was crystalline $\alpha\text{-Al}(\text{OH})_3$ in Fig. 1b. The water loss was 34.1 % between 240-600 °C in Fig. 2b. So the product was expressed as $\text{Al}_2\text{O}_3 \cdot 3.0\text{H}_2\text{O}$ ($\text{Al}(\text{OH})_3$). The precursor prepared by

reaction of HCl and NaAlO_2 was amorphous and was expressed as $\text{Al}_2\text{O}_3 \cdot 5.6\text{H}_2\text{O}$ from Fig. 1b.

Fig. 3 shows the morphologies of amorphous $\text{Al}_2\text{O}_3 \cdot 5.6\text{H}_2\text{O}$ (a) and crystalline $\text{Al}_2\text{O}_3 \cdot 3.0\text{H}_2\text{O}$ (b). Amorphous $\text{Al}_2\text{O}_3 \cdot 5.6\text{H}_2\text{O}$ had the structure of porous which determined they were easy to dissolve during the hydrothermal process. Fig. 3b shows the morphologies of $\text{Al}_2\text{O}_3 \cdot 3.0\text{H}_2\text{O}$ before and after acid treatment. $\text{Al}_2\text{O}_3 \cdot 3.0\text{H}_2\text{O}$ were spherical particles with ten microns in diameter, and their surface were made of sheet piles. After acid treatment ($2.0 \text{ mol} \cdot \text{L}^{-1}$ HCl for 2 h), schistose $\text{Al}_2\text{O}_3 \cdot 3.0\text{H}_2\text{O}$ were instead of spherical particles. We could infer that the acid immerse to the gap of the sheet piles, and dissolved connection of the sheet piles. Comparing with the spherical particles, the sheet piles left had greater surface area, and more likely to be dissolved in hydrothermal process.

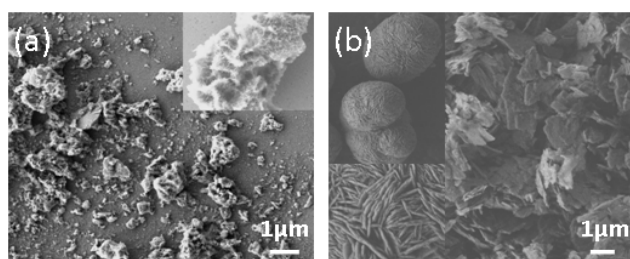


Figure 3. Morphology of hydrothermal precursors: (a) amorphous $\text{Al}_2\text{O}_3 \cdot 5.6\text{H}_2\text{O}$; (b) crystalline $\text{Al}_2\text{O}_3 \cdot 3.0\text{H}_2\text{O}$

3.2 Effect of mass ratio on morphology of AlOOH

The changes of AlOOH morphologies were shown in Fig. 4. The hydrothermal precursors were the mixture of $\text{Al}_2\text{O}_3 \cdot 5.6\text{H}_2\text{O}$ and $\text{Al}_2\text{O}_3 \cdot 3.0\text{H}_2\text{O}$ with different mass ratio. Using only $\text{Al}_2\text{O}_3 \cdot 5.6\text{H}_2\text{O}$ as precursor obtained AlOOH with a length of 400-600 nm and a diameter of 20-40 nm (Fig. 4a), while using $\text{Al}_2\text{O}_3 \cdot 3.0\text{H}_2\text{O}$ as precursor, no whisker appeared after hydrothermal treatment (Fig. 4f). When the mass ratio of $\text{Al}_2\text{O}_3 \cdot 5.6\text{H}_2\text{O}$ to $\text{Al}_2\text{O}_3 \cdot 3.0\text{H}_2\text{O}$ was between 2:1 and 1:2, AlOOH whiskers with a length of 800-1500 nm and a diameter of 20-40 nm were formed (Fig. 4b, c, d, e). Fig. 4a and Fig. 4f indicated that amorphous $\text{Al}_2\text{O}_3 \cdot 5.6\text{H}_2\text{O}$ dissolved and formed crystals again orienting to one dimensional direction, while the product of crystalline $\text{Al}_2\text{O}_3 \cdot 3.0\text{H}_2\text{O}$ was no specific growth direction. So they played different roles in hydrothermal process. Amorphous $\text{Al}_2\text{O}_3 \cdot 5.6\text{H}_2\text{O}$ was more likely to be an inducer and template which formed crystal with one-dimensional morphology firstly, crystalline $\text{Al}_2\text{O}_3 \cdot 3.0\text{H}_2\text{O}$ was dissolved to improve the content of solution Al^{3+} . The addition of crystalline $\text{Al}_2\text{O}_3 \cdot 3.0\text{H}_2\text{O}$ was limited by saturation degree of hydrothermal solution. In Fig. 4e, the AlOOH whiskers were mixed with some particles which were likely to result by the excessive $\text{Al}_2\text{O}_3 \cdot 3.0\text{H}_2\text{O}$.

3.3 Variation in hydrothermal process

Nano Biomed. Eng. 2010, 2, 121-125

The morphology changes of hydrated alumina were shown in Fig. 5. When the mass ratio of $\text{Al}_2\text{O}_3 \cdot 5.6\text{H}_2\text{O}$ to $\text{Al}_2\text{O}_3 \cdot 3.0\text{H}_2\text{O}$ was 1:1, small particles existed in half an hour and small whiskers appeared at 1h and kept long with time. The length of AlOOH was up to 400-500 nm till 2.0 h. When the mass ratio of $\text{Al}_2\text{O}_3 \cdot 5.6\text{H}_2\text{O}$ to $\text{Al}_2\text{O}_3 \cdot 3.0\text{H}_2\text{O}$ was 1:0, small whiskers with the length of 100-200 nm obtained at 2.0 h. The length of AlOOH was significant different between the two in the early reaction. The particles in Fig. 5a and Fig. 5b could not be distinguished between $\text{Al}_2\text{O}_3 \cdot 5.6\text{H}_2\text{O}$ and $\text{Al}_2\text{O}_3 \cdot 3.0\text{H}_2\text{O}$. But we can clearly see that there were particles in Fig. 5c and Fig. 5d, but only whiskers left in Fig. 5e and Fig. 5f. That told us amorphous $\text{Al}_2\text{O}_3 \cdot 5.6\text{H}_2\text{O}$ dissolved within 1.0h by hydrothermal treatment, while $\text{Al}_2\text{O}_3 \cdot 3.0\text{H}_2\text{O}$ needed more time to transform.

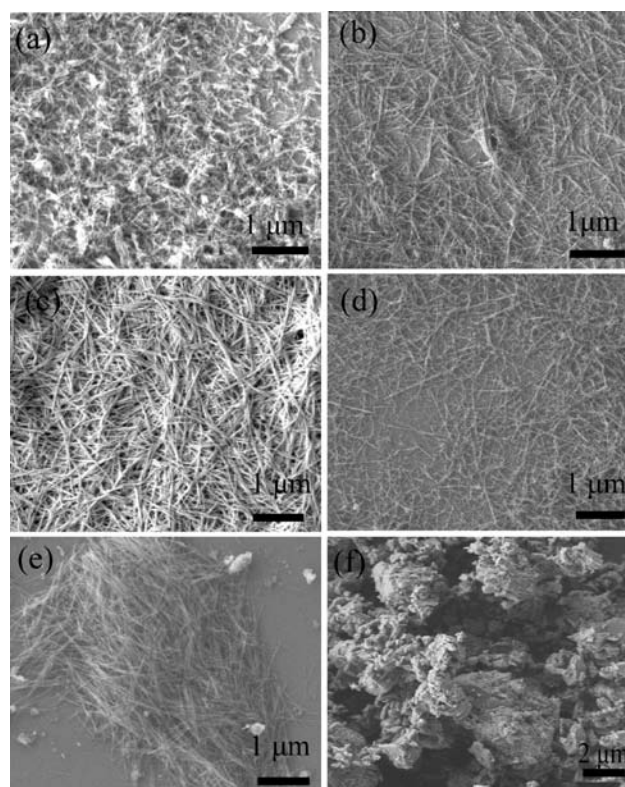


Figure 4. Morphology of the AlO(OH) whiskers formed with different mass ratio of $\text{Al}_2\text{O}_3 \cdot 5.6\text{H}_2\text{O}$ to $\text{Al}_2\text{O}_3 \cdot 3.0\text{H}_2\text{O}$: a, 1:0; b, 2:1; c, 1:1; d, 1:2; e, 1:4; f, 0:1

Fig. 6 shows the variation of the Al^{3+} ion with mass ratio of $\text{Al}_2\text{O}_3 \cdot 5.6\text{H}_2\text{O}$ to $\text{Al}(\text{OH})_3$ were 1:0 and 1:1 in hydrothermal process. The total aluminum concentration that only amorphous $\text{Al}_2\text{O}_3 \cdot 5.6\text{H}_2\text{O}$ as the precursor increased largely at first due to the dissolution of amorphous $\text{Al}_2\text{O}_3 \cdot 5.6\text{H}_2\text{O}$. Up to a certain concentration, the ions formed nucleuses which had marked tendency to grow along one-dimensional direction. Nucleation consumed aluminum concentration, so the total aluminum concentration decreased quickly and stabi-

lized at a very low level which provided the driving force of the growth of AlOOH crystal, as Fig. 5a shown. When the mass ratio of the two precursors was 1:1, the solution Al^{3+} ion followed the similar trend as former. The difference was the aluminum concentration in solution was significantly higher after hydrothermal treatment 30 min. The reason caused this change was due to crystalline $\text{Al}_2\text{O}_3 \cdot 3.0\text{H}_2\text{O}$. We knew that inorganic dissolution rate was usually affected by their crystallinity. $\text{Al}_2\text{O}_3 \cdot 5.6\text{H}_2\text{O}$ and $\text{Al}_2\text{O}_3 \cdot 3.0\text{H}_2\text{O}$ had different crystallinity which had been discussed above, so the dissolution of the two were not synchronized. Amorphous $\text{Al}_2\text{O}_3 \cdot 5.6\text{H}_2\text{O}$ dissolved firstly and crystalline $\text{Al}_2\text{O}_3 \cdot 3.0\text{H}_2\text{O}$ followed.

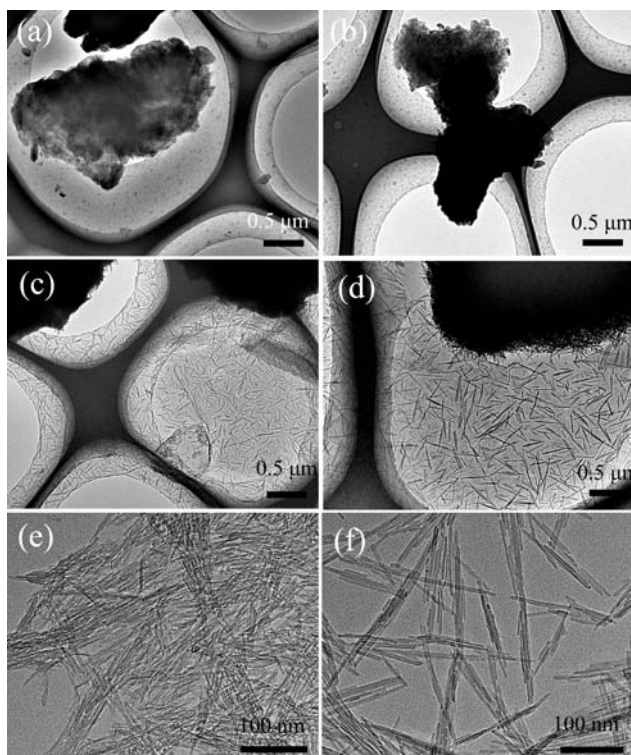


Figure 5. Variation of hydrated alumina with hydrothermal reaction time mass ratio of $\text{Al}_2\text{O}_3 \cdot 5.6\text{H}_2\text{O}$ to $\text{Al}(\text{OH})_3 = 1:1$: a, 15 min; b, 30 min; c, 60 min; d, 120 min; mass ratio of $\text{Al}_2\text{O}_3 \cdot 5.6\text{H}_2\text{O}$ to $\text{Al}(\text{OH})_3 = 1:0$: a, 60 min; b, 120 min

The point was clearly that increasing aluminum concentration in growth period of AlOOH crystal could help one-dimensional growth of AlOOH. Crystal theory told us the high aspect ratio of whiskers obtained under low supersaturation, while higher aluminum concentration got longer AlOOH whisker in our experiment. Despite the critical supersaturation of AlOOH was difficult to measure due to the closed system, we could infer that the solution was not saturated in dynamics. Increasing solution concentration was increasing the solution supersaturation, that was the reason why high aspect ratio was obtained when the

amorphous $\text{Al}_2\text{O}_3 \cdot 5.6\text{H}_2\text{O}$ mixed with crystalline $\text{Al}_2\text{O}_3 \cdot 3.0\text{H}_2\text{O}$.

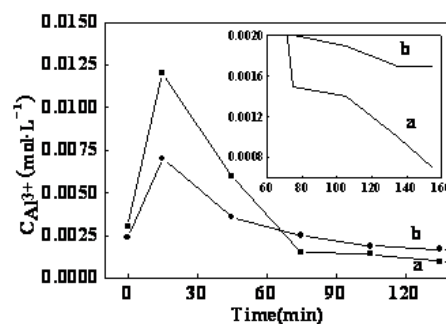


Figure 6. Variation of the Al^{3+} ion with hydrothermal reaction time mass ratio of $\text{Al}_2\text{O}_3 \cdot 5.6\text{H}_2\text{O}$ to $\text{Al}_2\text{O}_3 \cdot 3.0\text{H}_2\text{O}$: a, 1:0; b, 1:1

4. Conclusions

The properties of hydrated alumina precursors formed by different condition existed obvious differences and the roles of the two were different too in hydrothermal process. The acid-base neutralization of NaAlO_2 solution and NaOH solution obtained amorphous $\text{Al}_2\text{O}_3 \cdot 5.6\text{H}_2\text{O}$ which dissolved quickly to release Al^{3+} to form small crystal with one-dimensional morphology in the initial stage. The decomposition of NaAlO_2 solution got crystalline $\text{Al}(\text{OH})_3$ which dissolved to release Al^{3+} to stable concentration of Al^{3+} in the solution in the latter stage. The mixed of amorphous $\text{Al}_2\text{O}_3 \cdot 5.6\text{H}_2\text{O}$ and $\text{Al}(\text{OH})_3$ could stable concentration of Al^{3+} in the solution, which promoted the formation of the one-dimensional growth of γ -AlOOH whiskers.

Acknowledgments

The work was supported by the National Science Foundation of China (Grant No. 50874066) and the Open Foundation of Tsinghua University.

References

- Schreiner M, Wruss W, Lux B. Growth morphology and growth mechanism of α - Al_2O_3 whiskers. *Journal of Crystal Growth* 1983, 61: 75-79. [doi:10.1016/0022-0248\(83\)90281-6](https://doi.org/10.1016/0022-0248(83)90281-6)
- Chandradass J, Bae DS, Balasubramanian M. Synthesis and characterization of sol-gel alumina fiber by seeding alpha-alumina through extended ball milling. *Materials and Manufacturing Processes* 2008, 23(8): 786-790. [doi:10.1080/10426910802382098](https://doi.org/10.1080/10426910802382098)
- Bao YH, Nicholson PS. AlPO_4 -coated mullite/alumina fiber reinforced reaction-bonded mullite composites. *Journal of the European Ceramic Society* 2008, 28(16): 3041-3048. [doi:10.1016/j.jeurceramsoc.2008.05.032](https://doi.org/10.1016/j.jeurceramsoc.2008.05.032)
- Kaya C, He JY, Gu X, et al. Nanostructured ceramic powders by hydrothermal synthesis and their applications.

- Microporous Mesoporous Materials, 2002, 54: 37-49. [doi:10.1016/S1387-1811\(02\)00334-7](https://doi.org/10.1016/S1387-1811(02)00334-7)
5. Zhu HY, Riches JD, Barry JC. Gamma-alumina nanofibers prepared from aluminum hydrate with poly ethylene oxide surfactant. Chemistry of Materials, 2002, 14(5): 2086-2093. [doi:10.1021/cm010736a](https://doi.org/10.1021/cm010736a)
 6. Mathieu Y, Lebeau B, Valtchev V, Control of the morphology and particle size of boehmite nanoparticles synthesized under hydrothermal conditions. Langmuir, 2007, 23(18): 9435-9442. [doi:10.1021/la700233g](https://doi.org/10.1021/la700233g)
 7. He J, Clive B P. Hydrothermal synthesis and morphology control of boehmite. High Pressure Research, 2001, 20(1-6):241-254. [doi:10.1080/08957950108206171](https://doi.org/10.1080/08957950108206171)
 8. Chen XY, Lee SW. pH-dependent formation of boehmite (gamma-AlOOH) nanorods and nanoflakes. Chemical Physics Letters, 2007, 38: 279-284. [doi:10.1016/j.cpl.2007.03.020](https://doi.org/10.1016/j.cpl.2007.03.020)
 9. He T, Xiang L, Zhu W. H₂SO₄-assisted hydrothermal preparation of γ -AlOOH nanorods. Materials Letters, 2008, 62: 2939-2942. [doi:10.1016/j.matlet.2008.01.078](https://doi.org/10.1016/j.matlet.2008.01.078)
 10. He T, Xiang L, Zhu S. Hydrothermal Preparation of Boehmite Nanorods by Selective Adsorption of Sulfate. Langmuir, 2008, 24 : 8284-8289. [doi:10.1021/la8008514](https://doi.org/10.1021/la8008514)

Received 10 June, 2010; accepted 28 June, 2010; published online 1 July, 2010.

Copyright: (C) 2010 M. Chen et al. This is an open access article distributed under the terms of the Creative Commons Attribution License, which permits unrestricted use, distribution, and reproduction in any medium, provided the original author and source are credited.